

# Energy & Environmental Science

Accepted Manuscript



This is an *Accepted Manuscript*, which has been through the Royal Society of Chemistry peer review process and has been accepted for publication.

*Accepted Manuscripts* are published online shortly after acceptance, before technical editing, formatting and proof reading. Using this free service, authors can make their results available to the community, in citable form, before we publish the edited article. We will replace this *Accepted Manuscript* with the edited and formatted *Advance Article* as soon as it is available.

You can find more information about *Accepted Manuscripts* in the [Information for Authors](#).

Please note that technical editing may introduce minor changes to the text and/or graphics, which may alter content. The journal's standard [Terms & Conditions](#) and the [Ethical guidelines](#) still apply. In no event shall the Royal Society of Chemistry be held responsible for any errors or omissions in this *Accepted Manuscript* or any consequences arising from the use of any information it contains.

1 Date: January 27, 2014  
2 Submitted to: *Energy & Environmental Science*

3

4 **Capacitive Mixing Power Production from Salinity Gradient Energy**  
5 **Enhanced through Exoelectrogen-Generated Ionic Currents**

6

7 Marta C. Hatzell,<sup>1</sup> Roland D. Cusick,<sup>2</sup> and Bruce E. Logan<sup>2\*</sup>

8

9 <sup>1</sup> Department of Mechanical and Nuclear Engineering, The Pennsylvania State  
10 University, University Park, PA 16802, USA.

11 <sup>2</sup> Department of Civil and Environmental Engineering, 131 Sackett Building,  
12 The Pennsylvania State University, University Park, PA 16802, USA.

13

14 \*Corresponding Author: E-mail: [blogan@psu.edu](mailto:blogan@psu.edu); phone: +1-814-863-7908

15

16

17 Several approaches to generate electrical power directly from salinity gradient energy  
18 using capacitive electrodes have recently been developed, but power densities have  
19 remained low. By immersing the capacitive electrodes in ionic fields generated by  
20 exoelectrogenic microorganisms in bioelectrochemical reactors, we found that energy  
21 capture using synthetic river and seawater could be increased ~65 times, and power  
22 generation ~46 times. Favorable electrochemical reactions due to microbial oxidation of  
23 organic matter, coupled to oxygen reduction at the cathode, created an ionic flow field  
24 that enabled more effective passive charging of the capacitive electrodes and higher  
25 energy capture. This ionic-based approach is not limited to the use of river water-  
26 seawater solutions. It can also be applied in industrial settings, as demonstrated using  
27 thermolytic solutions that can be used to capture waste heat energy as salinity gradient  
28 energy. Forced charging of the capacitive electrodes, using energy generated by the

29 bioelectrochemical system and a thermolytic solution, further increased the maximum  
30 power density to  $7 \text{ W m}^{-2}$  (capacitive electrode).

31

## 32 **Introduction**

33 Harnessing the entropic energy released when river and seawater mix could globally  
34 provide  $\sim 1$  terrawatt of renewable power<sup>[1]</sup>. To capture this energy, three main  
35 processes have been used: pressure retarded osmosis (PRO)<sup>[2]</sup>, reverse electrodialysis  
36 (RED)<sup>[3]</sup>, and capacitive mixing (CapMix)<sup>[4]</sup>. These three processes are based on reversing  
37 three common approaches used to desalinate water, which are reverse osmosis,  
38 electrodialysis, and capacitive deionization. Industrial scale PRO and RED applications  
39 have been limited primarily due to relatively high energy requirements for river water  
40 and seawater pretreatment, high costs of membranes, and reduced lifetimes due to  
41 fouling<sup>[1, 5-7]</sup>. The CapMix approach to extract salinity gradient energy is based on  
42 controlled ion transfer to and from capacitive or battery electrodes. Suitable materials  
43 for energy generation using battery electrodes have not sufficiently advanced as  
44 precious metals (e.g. Ag) can be required<sup>[8]</sup>. In contrast, capacitive electrodes (high  
45 surface area) can be made from materials that are both renewable and inexpensive  
46 (such as activated carbon), and they can have longer lifetimes than battery electrodes<sup>[4,</sup>  
47 <sup>9, 10]</sup>.

48 CapMix energy is captured by cycles of charging and discharging capacitive  
49 electrodes with seawater and river water. The energy can be captured with these  
50 capacitive electrodes two different ways: either through changes in membrane

51 potentials due to ion concentration gradients<sup>[9, 11-13]</sup>; or through work done by  
52 expansion of the electric double layer. For energy recovery based on changes in the  
53 membrane potentials (also called Donnan potentials), the capacitive electrodes are  
54 coated with ion exchange polymers that allow only selective charge transfer (anions or  
55 cations) to each of the electrodes. Energy captured using this capacitive Donnan  
56 potential (CDP) approach requires cycles that consist of four separate steps (Fig. 1a).  
57 Initially, under open circuit conditions, the capacitive electrodes are polarized using a  
58 high concentrate solution (seawater) due to the generation of a membrane potential at  
59 each electrode (Step 1). Next, the capacitive electrodes are connected to an external  
60 load which allows the flow of electrical current through a circuit, and ionic current in the  
61 electrolyte (Step 2). Once the capacitive electrodes are fully charged (voltage  $U = 0$ ), the  
62 circuit is again opened (no current) and a low concentrate solution (river water) is  
63 introduced, reversing the polarity of each membrane potential (Step 3). The electrodes  
64 are then connected to an external load and discharged, creating an electrical current in  
65 the opposite direction (Step 4). The net energy that is extracted is defined by the  
66 voltage window produced by the membrane potential (Fig 1b). This four step CDP cycle  
67 results in spontaneous energy generation, and therefore the process does not require  
68 any electrical input energy. However, the potential energy,  $E$ , that can be recovered is  
69 limited as only a relatively small voltage (<100 mV) can be produced by the membrane  
70 potential alone ( $E = \frac{1}{2}CU^2$ , where  $U$  is the voltage, and  $C$  is the capacitance).

71 To increase the amount of energy recovered from this four step cycle, an external  
72 power supply is used in Step 2 to increase the charge loaded onto the membrane-

73 coated electrodes (called forced CDP) (see Fig 1b). While the use of the power source  
74 requires additional energy to be put into the system, the forced charging step increases  
75 the size of the voltage window. As long as there is no substantial charge leakage<sup>[14]</sup> (i.e.  
76 coulombic losses during the charging step), the current extracted in Step 4 (at a higher  
77 voltage) enables increased energy recovery, as shown by the larger voltage window (Fig  
78 1b). Thus, the peak power density that can be obtained using forced CDP has been  
79 increased to an average of 200 mW per square meter of electrode area<sup>[14]</sup>, compared to  
80 20-40 mW m<sup>-2</sup> using (passive) CDP<sup>[9, 11]</sup> However, even these higher power densities for  
81 forced CDP are still well below those reported for RED (0.95-1.2 W m<sup>-2</sup>-membrane area)  
82<sup>[15, 16]</sup> or PRO (1-10 W m<sup>-2</sup>-membrane area)<sup>[17, 18]</sup>. Thus, this technology will not be useful  
83 for energy generation until power densities can be substantially improved.

84 One approach recently used to increase energy recovery from salinity gradients  
85 using RED was incorporating the RED stack of membranes into a bioelectrochemical  
86 system, such a microbial fuel cell (MFC). The combination of these two technologies  
87 enabled significant improvements in performance for both technologies<sup>[19-21]</sup>. The RED  
88 process was improved because the reactions at the MFC electrodes were  
89 thermodynamically favorable, thereby avoiding energy losses needed to overcome  
90 unfavorable reactions usually occurring with RED alone. The MFC process was improved  
91 due to the reduced electrode overpotentials that resulted from the ionic current that  
92 was driven by the RED stack<sup>[20, 22]</sup>. The combination of these two technologies thus  
93 created a more effective means to harvest both free energy associated with the salinity  
94 gradients, as well as energy in a domestic wastewater (1-2 kWh per m<sup>3</sup> of wastewater

95 <sup>[23]</sup>). The success in combining salinity gradient and bioelectrochemical technologies  
96 suggested that it might be possible to improve performance of the other salinity  
97 gradient energy technologies by using MFCs.

98 A new method was developed here to increase CDP performance by placing the  
99 capacitive electrodes into the ionic field generated in a galvanostatically driven  
100 bioelectrochemical system (BES) (Fig 2a). When exoelectrogenic bacteria oxidize organic  
101 matter and release electrons to the anode in a BES such as an MFC, ions (protons) are  
102 released into the electrolyte, and protons are consumed at the cathode <sup>[24]</sup>. In order to  
103 maintain electroneutrality, an electric field drives ionic currents in the solution either  
104 through the motion of protons or by transport of other ionic species <sup>[19, 20, 25]</sup>. It was  
105 reasoned that immersion of capacitive electrodes into this ionic field could enhance  
106 charging of these capacitive electrodes, and enable increased power densities through  
107 the CapMix process. The combined process could then be used capture energy both  
108 from salinity gradients and organic matter in wastewater with the BES.

109 The energy and power produced from both the CDP, and combined CDP-BES  
110 process, was examined here to show that ionic fluxes from the BES could improve the  
111 CapMix process. In addition to tests using synthetic seawater and river water solutions  
112 (NaCl), the potential use of recyclable thermolytic salts (ammonium bicarbonate, AmB)  
113 was also examined. Capacitive energy extraction so far has only been investigated using  
114 NaCl solutions, which would limit applications to coastal regions. The use of thermolytic  
115 solutions enables closed loop operation using waste heat, with conventional distillation  
116 processes for solution regeneration. Industrial waste heat accounts for between 20-50%

117 of industrial energy input<sup>[26]</sup>, and capturing this energy using AmB would allow for  
118 power generation at industrial sites where it could readily be used. Both conventional  
119 CDP and forced CDP processes were investigated for improving performance of CapMix  
120 systems with AmB and NaCl solutions.

121

## 122 **Materials and Methods**

### 123 *Capacitive mixing bioelectrochemical system design*

124 The combined CapMix and BES system, called a capacitive mixing bioelectrochemical  
125 system (CBES), consisted of three chambers: anolyte, CapMix, and catholyte (Fig. 2a).  
126 The three chambers were separated from each other using two anion exchange  
127 membranes (AEMs). The use of the membranes allowed the solutions used for the two  
128 different processes to remain separated, while maintaining an ionic connection needed  
129 for the BES. The anolyte chamber was created from a 4 cm polycarbonate cube which  
130 had a 28 mL cylindrical chamber cut out. The CapMix (middle chamber) and catholyte  
131 chambers consisted of a 2 cm Lexan cube, each 14 mL with the same diameter  
132 cylindrical chambers. Brush anodes (manufactured by Mill-Rose, Mentor, OH) were  
133 made from graphite fibers twisted between two titanium wires (4 cm diameter). Anodes  
134 were heat treated and enriched in a vertical configuration within a single chamber  
135 MFCs, as previously described (26). When enrichment was complete the anode was  
136 transferred to the CBES anolyte chamber. The anolyte solution used in all tests was a 50  
137 mM phosphate buffer, 1 g l<sup>-1</sup> sodium acetate and trace vitamins and minerals.

138 Cathodes were made using wet proofed carbon cloth (type B, E-Tek) which was  
139 coated with carbon black, platinum ( $0.5 \text{ mg-Pt cm}^{-2}$ ) and a NAFION® 117 (Aldrich) binder  
140 on the water side<sup>[27]</sup>. The air side had 4 layers of polytetrafluoroethylene (PTFE) coatings  
141 which acted as diffusion layers to allow oxygen diffusion to the catalyst, and to  
142 prevent water leakage<sup>[28]</sup>. The catholyte solution consisted of the high concentrate  
143 saline solution, which was either 500 mM NaCl or  $\text{NH}_4\text{HCO}_3$  as indicated.

144 The capacitive electrodes were made using 90 wt.% YP-50F activated carbon  
145 (Kuraray Chemical Company, USA), 5 wt.% polytetrafluoroethylene as a binder, and 5  
146 wt.% carbon black (100% compressed; Alfa Aesar, USA) to increase electrode electrical  
147 conductivity. The resultant slurry was rolled and cut into square electrodes with an area  
148 of  $1 \text{ cm}^2$  and an approximate weight of 15 mg. During electrochemical characterization  
149 tests, the electrodes were placed on non-corrosive current collectors made of graphite  
150 foil. A polyvinylidene fluoride (PVDF) membrane separator with a mesh width of 100 nm  
151 (Durapore®; Merck Millipore, Germany) was used as the separator between the two  
152 electrodes. The entire cell was compressed between two PTFE plates with clips.

153 For CapMix tests the capacitive electrodes were hot pressed onto a current  
154 collector (SS mesh Type 316, McMaster-Carr). One coating of an anion exchange  
155 polymer (polysulfone polymer with quaternary ammonium groups)<sup>[29]</sup> was put onto one  
156 capacitive film electrode, and one coating of cation exchange polymer (NAFION® 117)  
157 polymer was put onto the other one. Both electrodes were dried overnight prior to use.  
158 These capacitive electrodes were placed on either side of the central CapMix chamber  
159 (2 cm apart). The capacitive electrode with the anion coating was placed against the



160 AEM membrane-anolyte interface, with the membrane coated capacitive electrode side  
161 facing the water side. The capacitive electrode with the cation coating was placed near  
162 the membrane-catholyte interface, with the membrane coated facing the water side of  
163 the CapMix chamber.

164

165 *Ex situ capacitive electrode electrochemical characterization*

166 The capacitive electrodes were electrochemically characterized in a symmetrical two  
167 electrode set-up (Fig. 1s). Cyclic voltammetry (CV) studies of the capacitive electrodes  
168 were performed using the two-electrode setup<sup>[30, 31]</sup>. CVs were run at different scan  
169 rates (2, 5, 10, 20, 50, 100 mV s<sup>-1</sup>) in the different aqueous media used here to assess  
170 their performance (Fig. 1s). From these CVs, the specific gravimetric  $C_{sp}$  was obtained  
171 using

$$C_{sp} = \frac{2}{\Delta U} \cdot \frac{\int idU}{\nu \cdot m} \quad (\text{Eq. 1})$$

172 where  $\Delta U$  is the width of the voltage scan,  $i$  is the discharge current,  $U$  is the voltage,  $\nu$  is  
173 the scan rate, and  $m$  is the mass of carbon in one electrode.

174

175 *BES system performance*

176 Whole cell polarization curves were conducted without capacitive electrodes  
177 present, with both high and low concentration solutions tested in CapMix experiments.  
178 Galvanostatic polarization curves were obtained using a Biologic Potentiostat (VMP3  
179 Multichannel Workstation, Biologic Science Instruments, USA). Current was stepped

180 between 0 mA to 9 mA (1 mA steps), and held for 10 minutes until steady state  
181 conditions were obtained (Fig. 2s). Ag/AgCl reference electrodes (BASi, West Lafayette,  
182 IN) were placed in the anolyte, CapMix and catholyte chambers to monitor electrode  
183 and membrane potentials, and to calculate the whole cell potential. Both power and  
184 current density for the BES were normalized against the total cathode area (7 cm<sup>2</sup>).

185

#### 186 *Capacitive mixing performance*

187 The CapMix (middle chamber) and BES (end chambers) were operated separately  
188 without any electrical connections between the two systems (Fig 2). The BES was  
189 operated by connecting the brush anode to the air breathing oxygen reduction cathode  
190 through an external load (controlled by the galvanostat). Likewise, the two capacitive  
191 electrodes within the CapMix chamber were connected to each other through a  
192 separate external load. Energy obtained through the BES circuit was due to the  
193 oxidation of organic matter (acetate), while energy harvested through the CapMix  
194 circuit was due to mixing energy.

195 The BES was operated under constant current conditions between 1-5 mA  
196 (galvanostatically), which was chosen to ensure that the BES potential was positive  
197 when both the high and low concentration solution was present within the CapMix  
198 chamber. Separate tests using a constant load (resistor) were also conducted to  
199 demonstrate that the use of the galvanostic operation for these tests did not produce  
200 different results than those under typical BES operation with a constant load (Fig. 3s and  
201 Fig. 3). Substrate removal in the BES was not monitored. While the BES electrodes were

202 maintained in a constant discharge mode using the galvanostat, the capacitive  
203 electrodes were repeatedly cycled through the four step CDP energy extraction process.  
204 Briefly, in Step 1, capacitive electrodes were polarized in the high concentration solution  
205 (NaCl or AmB) under open circuit conditions (Fig 4s–A). In Step 2 the capacitive  
206 electrodes were connected to a 10  $\Omega$  external resistance for 5 minutes, until the current  
207 through the circuit approached zero (Fig 4s–B). In Step 3, the capacitive electrodes were  
208 again disconnected (open circuit), and the high concentration solution was replaced by  
209 the low concentration solution (10 mM NaCl or AmB) (Fig 4s–C). After the electrode  
210 polarity switched due to the reversal of the membrane potential, in Step 4 the  
211 capacitive electrodes were discharged through a 100  $\Omega$  resistor for 20 minutes (Fig 4s–  
212 D). This cycle was repeated 5-10 times to ensure repeatability.

213 Voltages were converted to power density, and power density and current density  
214 were plotted versus time to evaluate the CapMix system performance using  $P =$   
215  $(UI)/A$  where here  $U$  is the voltage,  $I$  is the current, and  $A$  is the area of one biased  
216 electrode (1 cm<sup>2</sup>). Individual cycles were analyzed from the voltage and charge  
217 accumulation, with the energy extracted from each cycle calculated using the integral:

$$W = \frac{-\oint_c \Delta U dq}{m} \quad (\text{Eq. 2})$$

218 where  $\Delta U$  is the change in voltage,  $dq$  is the change in charge stored in the capacitors,  
219 and  $m$  is the mass of one electrode.

220

221 *Forced capacitive mixing performance*

222 Forced charge CDP experiments were conducted using the BES as the power source.  
223 All forced charge CDP tests used 500 mM and 10 mM AmB as the high and low  
224 concentrate solutions in the CapMix chamber, and 500 mM AmB as the catholyte in the  
225 BES. The same four step process described for CDP operation was used (Fig 1a), except  
226 that during Step 2 the BES electrodes were connected to the capacitive electrodes  
227 through a connecting wire (Fig. 1b). The BES electrodes were connected to the  
228 capacitors for 5 minutes, and current was monitored by measuring the voltage drop  
229 across a 10  $\Omega$  resistor. Next, the BES and capacitive electrodes were disconnected and  
230 the CapMix chamber was flushed with the low concentrate solution, reversing the  
231 membrane potential (Step 3). The capacitive electrodes were then discharged through  
232 an 800  $\Omega$  resistor for 1 hour to reduce the charge leakage (Step 4). During this time, the  
233 BES electrodes were connected to a 10  $\Omega$  resistor. After 1 hour, the capacitors were left  
234 in open circuit, and the low concentrate was replaced with a high concentrate. The cycle  
235 was repeated multiple times to ensure repeatability.

236

## 237 **Results and Discussion**

### 238 *Evaluating the effect of BES current on CapMix*

239 To demonstrate enhancement on CapMix by BES ionic currents, the capacitive  
240 electrodes were cycled multiple times through the four-step energy extraction process  
241 with the BES current set at 2 or 4 mA using NaCl solutions. The capacitive electrodes  
242 were charged for five minutes (10  $\Omega$  external resistance) in high concentration solution,  
243 and discharged for 20 minutes (100  $\Omega$  resistor) in low concentration solution. At 2 mA,

244 the peak voltage was  $114 \pm 4$  mV ( $n=3$ ), producing a maximum power density of  $232 \pm$   
245  $18$  mW m<sup>-2</sup> (average of  $44 \pm 4$  mW m<sup>-2</sup>) (Fig. 3). This is a 2.3× increase in voltage, and  
246 24× increase in maximum power compared to controls with no enhanced ionic current  
247 ( $35 \pm 0$  mV and  $9.6 \pm 0.3$  mW m<sup>-2</sup>; average of  $0.013 \pm 0.001$  mW m<sup>-2</sup>,  $n=4$ ). The low power  
248 density for the capacitive electrodes in the absence of the ionic current was consistent  
249 with previous reports (Table 1s). When the BES current was increased toward the  
250 limiting current that could be produced by this reactor ( $\sim 4$  mA), the peak power  
251 increased to  $448 \pm 67$  mW m<sup>-2</sup> ( $77 \pm 24$  mW m<sup>-2</sup> average), which was 11× more power  
252 than that previously obtained in CDP tests (no forced charging), and 46× that achieved  
253 with the same capacitive electrodes and no induced ionic current (Table 1s). Multiple  
254 CapMix cycles were possible because the length for a full CapMix cycle ( $\sim 30$  min) was  
255 substantially less than that needed for a single BES fed-batch cycle (16-18 hrs). A higher  
256 current might have further increased power densities produced by the CDP, but this was  
257 not possible with NaCl due to having reached the limiting current density (limited by  
258 internal resistance 60-80  $\Omega$ ). The reason for the increased performance of the CapMix  
259 process combined with the BES could only have been due to the ionic currents. Further  
260 background regarding the ionic currents or fluxes is provided in the Supporting  
261 Information.

262

### 263 *Evaluating the effect of BES current on CapMix energy extraction*

264 The energy extracted by CDP charging was calculated from the area inside the  
265 voltage versus charge accumulation curve over each cycle (Fig. 4). Energy recovery with

266 BES operation was  $59 \pm 10 \text{ mJ g}^{-1} \text{ cycle}^{-1}$  (2 mA) or  $175 \pm 16 \text{ mJ g}^{-1} \text{ cycle}^{-1}$  (4 mA),  
267 compared to only  $2.7 \pm 0.1 \text{ mJ g}^{-1} \text{ cycle}^{-1}$  for controls (no ionic current) (Fig. 4). The  
268 energy which can be extracted from the capacitive electrodes in the presence of an BES  
269 with a constant discharge of 2 mA is equivalent to nearly 19 cycles from the CDP process  
270 without an BES. When the BES was operated at 4 mA the energy extracted in one cycle  
271 was comparable to nearly 60 cycles without the BES. In addition to this energy extracted  
272 by the capacitive electrodes,  $\sim 200 - 300 \text{ mJ cycle}^{-1}$  was extracted from organic matter  
273 using the BES over its complete cycle.

274

#### 275 *Effect of CapMix on Microbial Fuel Cell Performance*

276 The operation of the three-chamber BES allowed for greater peak power densities  
277 than achievable in a single chamber BES (Fig 2s), however, the voltage and power  
278 fluctuated during the CDP four step process (Fig 5a &b). In particular, the performance  
279 decreased during Steps 2 and 3 due to the addition of a large resistance (low  
280 concentrate chamber). The BES's operational power at 4 mA decreased from  $1.41 \pm 0.03$   
281  $\text{W m}^{-2}$  (cathode) to  $0.44 \pm 0.09 \text{ W m}^{-2}$  (cathode) when the high concentration was  
282 replaced by the low concentration (NaCl). When the BES was operated at 2 mA, the BES  
283 power decreased from  $1.03 \pm 0.01 \text{ W m}^{-2}$  (cathode) to  $0.71 \pm 0.05 \text{ W m}^{-2}$  (cathode) (Fig  
284 5b). The intermittent addition of the low concentration solution was therefore  
285 detrimental to the BES operation, but necessary for CapMix power production. One way  
286 to reduce this resistance would be to design the system to have a thinner CapMix  
287 chamber.

288

289 *Capacitive mixing with thermolytic salts*

290 The performance of the CapMix electrodes was further examined using AmB high  
291 and low concentration solutions in the middle CapMix chamber, and a high  
292 concentration of AmB in the cathode chamber. The switch to AmB as the electrolyte did  
293 not significantly alter the capacitance of the electrodes compared to NaCl, with  $\sim 80$ - $90$  F  
294  $\text{g}^{-1}$  obtained for both electrolytes based on cyclic voltammetry tests ( $5 \text{ mV sec}^{-1}$  scan  
295 rate) (Fig. 1s). The use of AmB reduced cathodic resistance, increasing the systems  
296 limiting current ( $5 \text{ mA}$ ). At this higher current, the energy captured increased to  $314 \pm 27$   
297  $\text{mJ g}^{-1} \text{ cycle}^{-1}$  (Fig. 6), which was  $\sim 6\times$  more than that previously obtained using CDP. The  
298 increased limiting current with AmB compared to NaCl was due to the reduced  
299 overpotential of the cathode (Fig. 2s) because ammonium functions as a proton shuttle,  
300 which improves oxygen reduction. The cathode potential was therefore  $\sim 200 \text{ mV}$  higher  
301 at current densities in AmB than in NaCl.

302 Power densities for the CapMix electrodes with CDP charging using AmB reached  
303  $942 \pm 100 \text{ mW m}^{-2}$  (average  $301 \pm 87 \text{ mW m}^{-2}$ ), which approached levels previously  
304 obtained using only PRO, RED, or forced CDP processes. AmB increased the overall  
305 energy extracted through the CDP process relative to NaCl solutions. At a current of  $4$   
306  $\text{mA}$ ,  $244 \pm 30 \text{ mJ g}^{-1} \text{ cycle}^{-1}$  was extracted using AmB, compared to  $175 \pm 16 \text{ mJ g}^{-1}$   
307  $\text{cycle}^{-1}$  using NaCl. The advantage of the CapMix process compared to RED is that this  
308 power is extracted using only a pair of membranes, although the four-step charging  
309 cycle is more complex than that needed for RED operation. The advantage of CapMix

310 compared to PRO may be that membrane fouling is reduced as water does not need to  
311 flow through the membrane as it does in PRO.

312

313 *Forced charged CapMix using the BES*

314 Power generation and energy extraction using the CapMix process was further  
315 examined using the BES to directly charge the CDP electrodes in AmB. This forced  
316 charge method avoided the need for an external power source, as the power was  
317 provided directly by the BES. To force charge the CapMix electrodes, the BES anode was  
318 connected by a wire to the anion-coated capacitive electrode, and the cathode was  
319 connected to the cation-coated capacitive electrode. Forced charging increased the  
320 potential of the capacitive electrodes to  $\sim 0.65$  V after five minutes, which allowed  
321 increased energy extraction from the capacitive discharge process. The peak voltage  
322 increased from  $\sim 0.1$  V to  $\sim 0.85$  V (Fig. 7a), and peak power densities increased 8.5 $\times$  to  
323  $7.6 \pm 0.1$  W m<sup>-2</sup> ( $0.67 \pm 0.08$  W m<sup>-2</sup>, averaged over the discharge curve) compared to  
324 non-forced conditions (Fig. 7b). The energy extracted from the CapMix process  
325 increased 47 $\times$  to  $14,900 \pm 400$  mJ g<sup>-1</sup> cycle<sup>-1</sup>.

326 Power densities were further increased to 20 W m<sup>-2</sup> (capacitive electrode) when the  
327 discharge external load was reduced. However, at this lower external load the high rate  
328 of discharge caused an increase in leakage current, which reduced the net energy  
329 recovered (Fig. 7s). The charge obtained through the discharge was due solely to initially  
330 invested charge from the BES, and not from the CapMix process. When the charged  
331 capacitive electrodes were exposed to the low concentrate, the voltage increased from



332 0.5 V to nearly 0.75 V. However, when connected to an external load, the voltage of the  
333 capacitive electrodes immediately decreased to a voltage below that of the initial  
334 charge (0.5 V). Further optimization of materials and membranes to reduce charge  
335 leakage could therefore improve power densities using this approach.

336

### 337 **Conclusions**

338 Capacitive and battery-type electrode approaches offer novel methods for producing  
339 electrical power using naturally-occurring (seawater/river water) or engineered  
340 (thermolytic solution) salinity gradients. The use of an ionically driven current  
341 represents a new approach in the development of these technologies as it substantially  
342 increased power densities from  $\sim 10 \text{ mW m}^{-2}$  to  $\sim 500 \text{ mW m}^{-2}$  with NaCl, and  $\sim 900 \text{ mW}$   
343  $\text{m}^{-2}$  using thermolytic salts. The direct use of the BES electrodes to force charge the  
344 capacitive electrodes increased power densities further to  $\sim 7 \text{ W m}^{-2}$ . The combination  
345 of the bioelectrochemical and capacitive mixing processes could enable simultaneous  
346 wastewater treatment and provide a new method of power generation and energy  
347 recovery at either coastal or industrial sites.

348

### 349 **Acknowledgements**

350 This research was supported by the National Science Foundation Graduate Research  
351 Fellowship Program, and a grant from the King Abdullah University of Science and  
352 Technology (KAUST) (Award KUS-I1-003-13). We would like to acknowledge Guang  
353 Chen for synthesizing the AEM coating and Kelsey B. Hatzell for constructing and  
354 characterizing the capacitive electrodes.

355

356

357

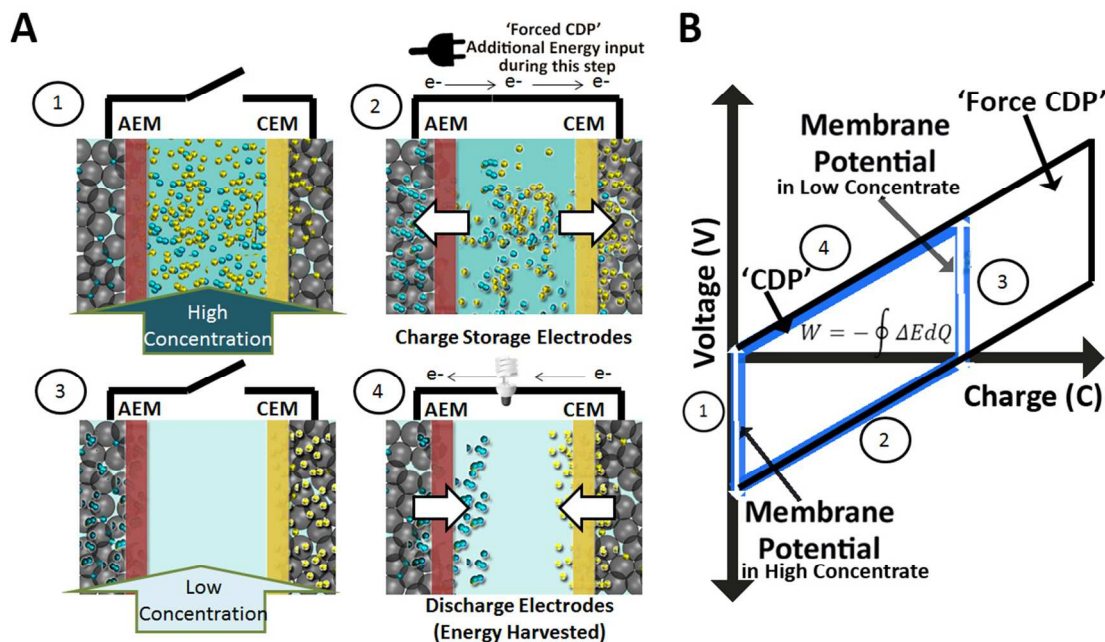
358

359

**References**

- 360 1. Ramon, G.Z., B.J. Feinberg, and E.M.V. Hoek, *Energy & Environmental Science*,  
361 **2011**, 4, 4423-4434.
- 362 2. Pattle, R.E., *Nature*, **1954**, 174, 660-660.
- 363 3. Weinstein, J.N. and F.B. Leitz, *Science*, **1976**, 191, 557.
- 364 4. Brogioli, D., *Physical Review Letters*, **2009**, 103, 058501.
- 365 5. Post, J., C. Goeting, J. Valk, S. Goinga, J. Veerman, H. Hamelers, and P. Hack,  
366 *Desalination and Water Treatment*, **2010**, 16, 182-193.
- 367 6. Vermaas, D.A., D. Kunteng, M. Saakes, and K. Nijmeijer, *Water research*, **2013**,  
368 47, 1289-1298.
- 369 7. Post, J.W., J. Veerman, H.V.M. Hamelers, G.J.W. Euverink, S.J. Metz, K.  
370 Nymeyjer, and C.J.N. Buisman, *Journal of Membrane Science*, **2007**, 288, 218-  
371 230.
- 372 8. La Mantia, F., M. Pasta, H.D. Deshazer, B.E. Logan, and Y. Cui, *Nano Letters*,  
373 **2011**, 11, 1810-1813.
- 374 9. Sales, B.B., M. Saakes, J.W. Post, C.J.N. Buisman, P.M. Biesheuvel, and H.V.M.  
375 Hamelers, *Environ. Sci. Technol.*, **2010**, 44, 5661-5665.
- 376 10. Simon, P. and Y. Gogotsi, *Nature Materials*, **2008**, 7, 845-854.
- 377 11. Sales, B.B., F. Liu, O. Schaetzle, C.J.N. Buisman, and H.V.M. Hamelers,  
378 *Electrochimica Acta*, **2012**, 86, 298-304.
- 379 12. Burheim, O.S., F. Liu, B.B. Sales, O. Schaetzle, C.J. Buisman, and H.V.  
380 Hamelers, *J. Phys. Chem. C*, **2012**, 116, 19203-19210.
- 381 13. Sales, B.B., O.S. Burheim, F. Liu, O. Schaetzle, C.J. Buisman, and H.V.  
382 Hamelers, *Environ. Sci. Technol.*, **2012**, 46, 12203-12208.
- 383 14. Liu, F., O. Schaetzle, B.B. Sales, M. Saakes, C.J. Buisman, and H.V. Hamelers,  
384 *Energy & Environmental Science*, **2012**, 5, 8642-8650.
- 385 15. Veerman, J., J. Post, M. Saakes, S. Metz, and G. Harmsen, *Journal of Membrane*  
386 *Science*, **2008**, 310, 418-430.
- 387 16. Veerman, J., M. Saakes, S. Metz, and G. Harmsen, *Journal of Membrane Science*,  
388 **2009**, 327, 136-144.
- 389 17. Chou, S., R. Wang, L. Shi, Q. She, C. Tang, and A.G. Fane, *Journal of Membrane*  
390 *Science*, **2012**, 389, 25-33.
- 391 18. Achilli, A., T.Y. Cath, and A.E. Childress, *Journal of Membrane Science*, **2009**,  
392 343, 42-52.
- 393 19. Kim, Y. and B.E. Logan, *PNAS*, **2011**, 108, 16176-16181.
- 394 20. Cusick, R.D., Y. Kim, and B.E. Logan, *Science*, **2012**, 335, 1474-1477.
- 395 21. Nam, J.Y., R.D. Cusick, Y. Kim, and B.E. Logan, *Environmental Science and*  
396 *Technology*, **2012**, 46, 5240-5246.
- 397 22. Kim, Y. and B.E. Logan, *Environmental science & technology*, **2011**, 45, 5834-  
398 5839.
- 399 23. McCarty, P.L., J. Bae, and J. Kim, *Environmental Science & Technology*, **2011**,  
400 45, 7100-7106.
- 401 24. Logan, B.E., *Nat Rev Micro*, **2009**, 7, 375-381.

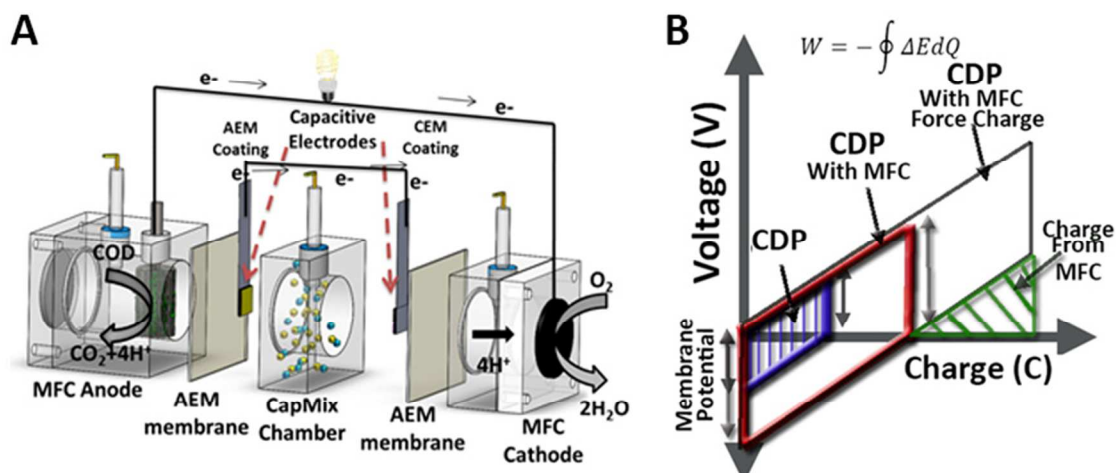
- 402 25. Logan, B.E. and K. Rabaey, *Science*, **2012**, 337, 686-690.
- 403 26. Johnson, I. and W.T. Choate *Waste Heat Recovery: Technology and*  
404 *Opportunities in the U.S. Industry*. 2008.
- 405 27. Cheng, S., H. Liu, and B.E. Logan, *Electrochemistry Communications*, **2006**, 8,  
406 489-494.
- 407 28. Liu, H. and B.E. Logan, *Environ. Sci. Technol.* , **2004**, 38, 4040-4046.
- 408 29. Chen, G., B. Wei, B.E. Logan, and M.A. Hickner, *RSC Advances*, **2012**, 2, 5856-  
409 5862.
- 410 30. Hatzell, K.B., M. Beidaghi, J.W. Campos, C.R. Dennison, E.C. Kumbur, and Y.  
411 Gogotsi, *Electrochimica Acta*, **2013**.
- 412 31. Campos, J.W., M. Beidaghi, K.B. Hatzell, C.R. Dennison, B. Musci, V. Presser,  
413 E.C. Kumbur, and Y. Gogotsi, *Electrochimica Acta*, **2013**.
- 414
- 415
- 416

417  
418419  
420

**Fig. 1:** (a) The four step process for capacitive mixing based on a membrane potential with open circuit and closed circuit condition and ion flux indicated. The individual steps (1 through 4) are explained in the text. Negatively charged ions move through the anion exchange membrane (AEM) to charge the anode, while the positively charged ions (yellow) travel through the cation exchange membrane (CEM) to charge the cathode. Note the circuit is opened when changing out the solutions from high to low concentration. The plug shown in step 2 indicates energy can be input into the system during a forced CDP charging step, while the light bulb indicates that energy is extracted in this step 4. (b) Voltage versus charge plot for the four step process, with each step and membrane potentials indicated. The work done over the four-step cycle is represented by the area enclosed by the blue outline (referred to here as the voltage window). In the forced charge mode, this area can be expanded to increase energy recovery.

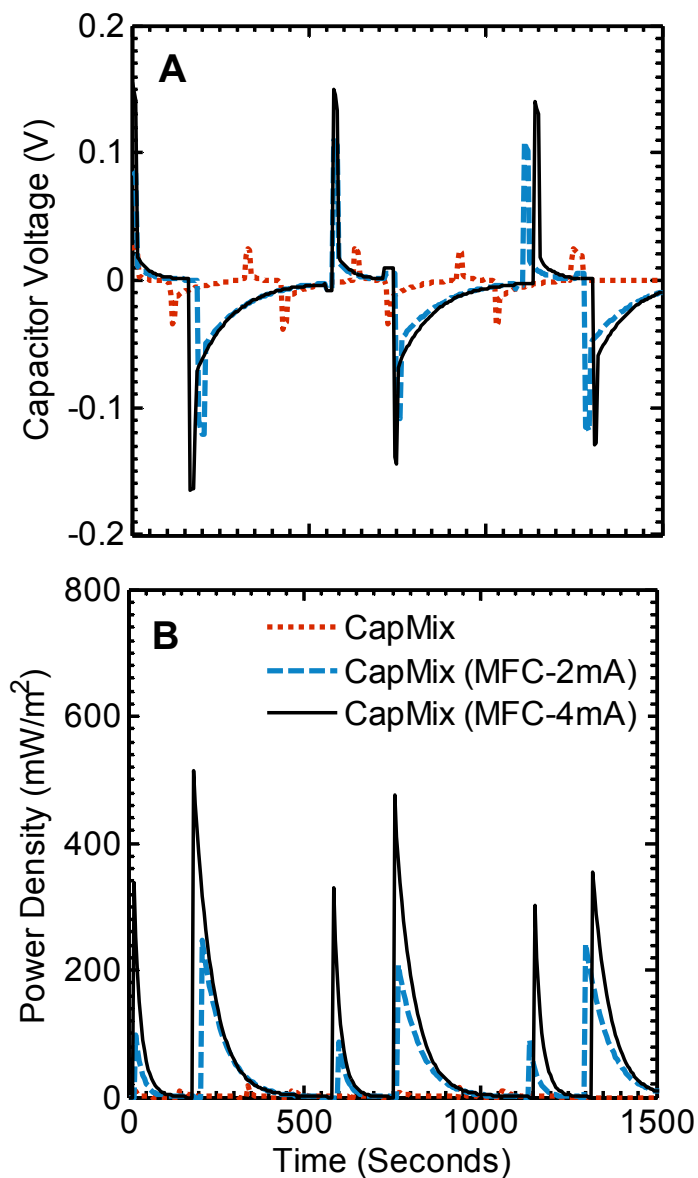
434  
435  
436  
437  
438  
439  
440  
441  
442  
443  
444

445  
446



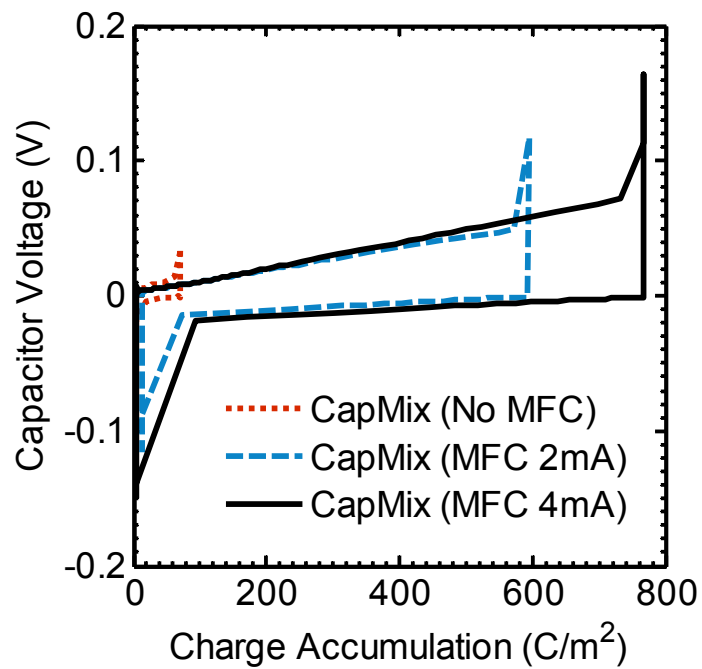
447  
448  
449  
450  
451  
452  
453  
454  
455  
456

**Fig 2.** a) CBES showing reactor components and electrode reactions. Note that the BES and the capacitive electrodes are operated using two separate electrical circuits. The solution in the CapMix middle chamber is changed using the four step cycle (see details in Fig 1a) while the BES operation over that period of time is continuous. b) Energy extracted from CDP (smaller blue lined area), compared to higher energy that can be extract using the CDP placed into the BES (red lines), and energy recovered forced charge CDP approach in an BES (grey lines).



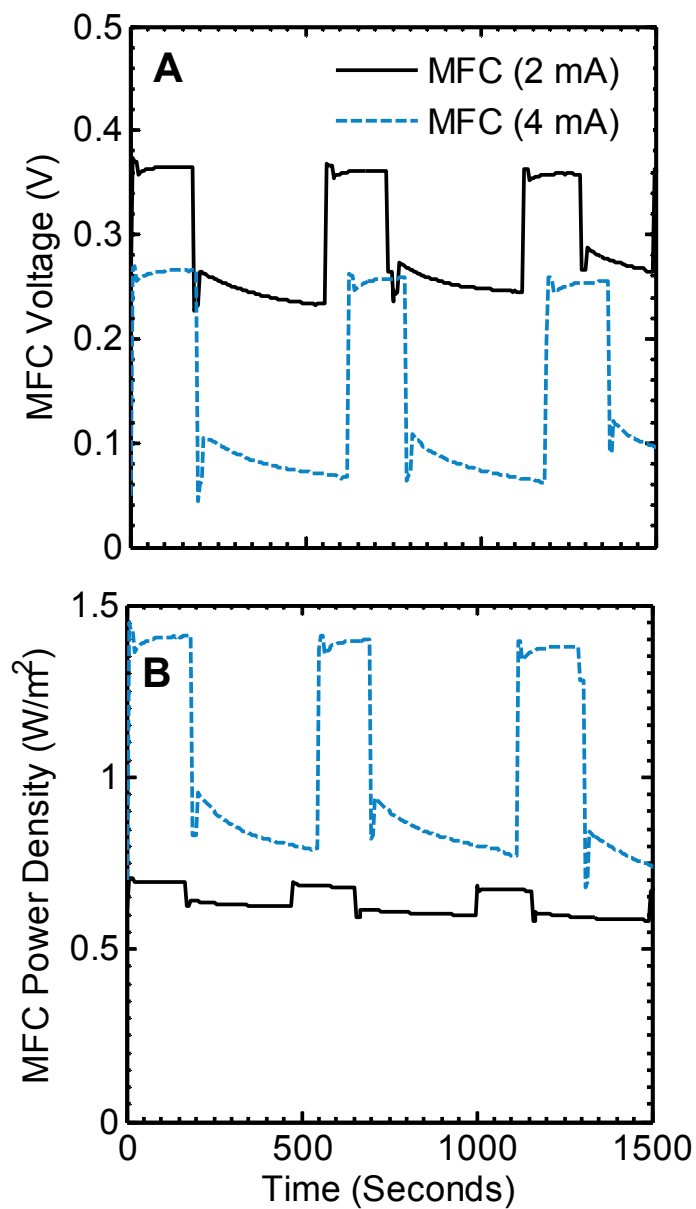
457  
458  
459  
460  
461  
462  
463  
464

**Fig. 3:** Capacitive mixing chamber performance with the BES operated at constant current at 2 mA or 4 mA, compared to CapMix alone. (a) Voltages produced during the four step charging-discharging CapMix process; and (b) power density produced (normalized per m<sup>2</sup> of one capacitive electrode).



465  
466  
467  
468  
469

**Fig. 4:** Energy extracted from CapMix and CapMix- BES system is defined as the area inside the voltage-charge cycle.



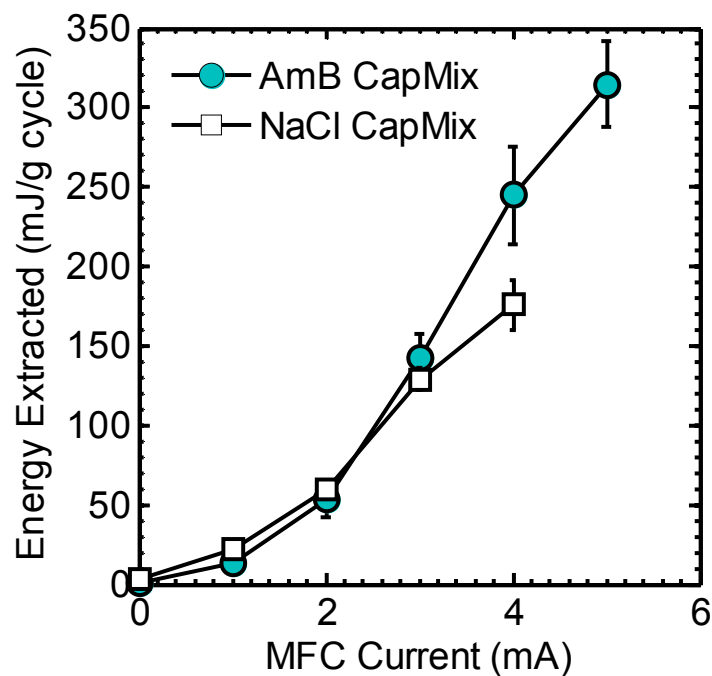
470

471 **Fig. 5:** Performance of the BES during the four-step CapMix cycles: (a) voltage and (b)  
472 power density (normalized per  $\text{m}^2$  of BES cathode).

473

474

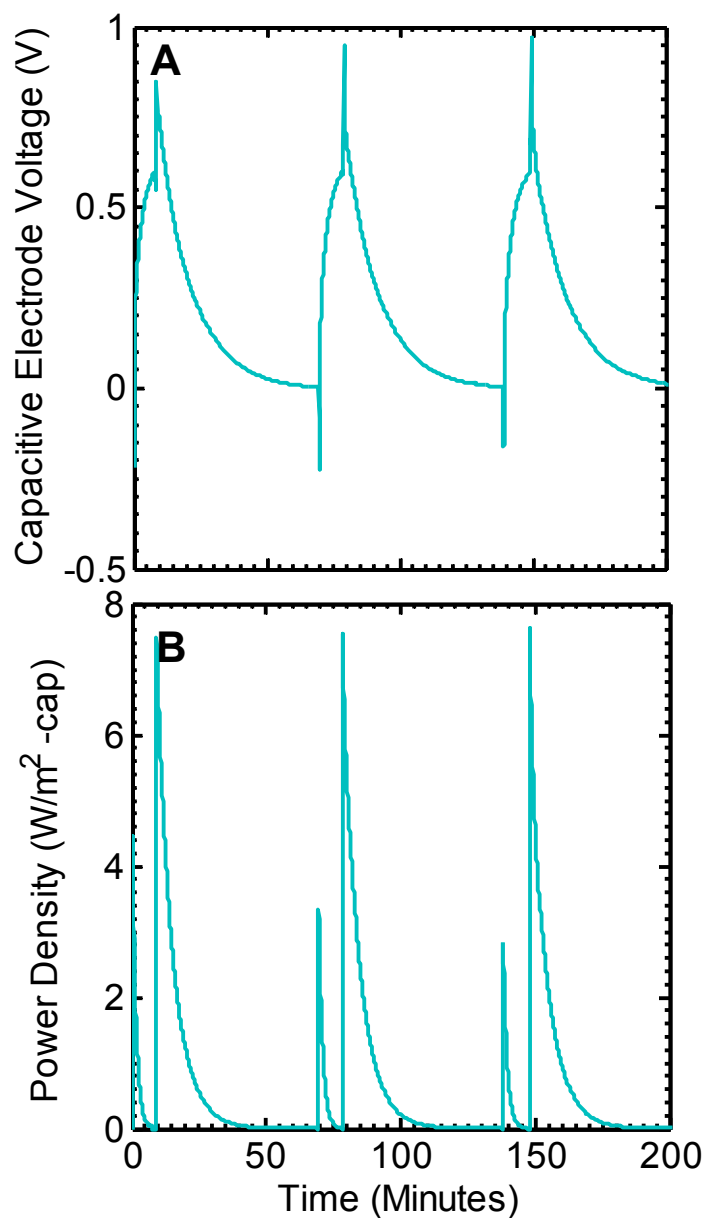




475  
476  
477  
478  
479  
480

**Fig. 6:** Total energy extracted with the BES set at different fixed currents using high (500 mM) and low (10 mM) concentration solutions of ammonium bicarbonate (AmB) or sodium chloride (NaCl) in the CapMix chamber. Energy extracted was normalized per gram of capacitive electrode.

481



482

483

484

485

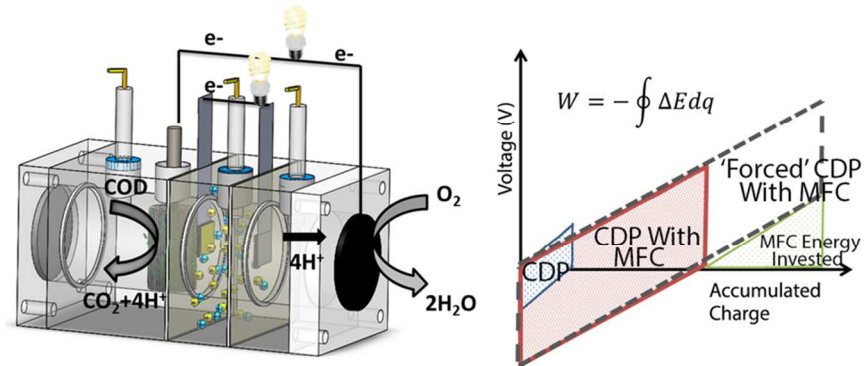
486

**Fig. 7:** Performance of the capacitive electrodes with forced charging using the BES: (a) capacitive electrode voltage; and (b) power densities (normalized to a single capacitive electrode area).

487 **Broader Context (<200 words)**

488 There is currently an enormous amount of free energy released through the mixing of  
489 river and seawater at estuaries. Furthermore, an abundance of untapped energy is also  
490 known to reside within organic matter present in many wastewaters. With a growing  
491 emphasis placed on mitigating the dependence between our expanding water and  
492 energy infrastructures across the globe, the development of sustainable dual energy  
493 generation and water treatment process is highly desirable. A combined capacitive  
494 mixing – microbial fuel cell could not only harvest this energy, but ultimately provide a  
495 new means for energy generation and wastewater treatment.

## Graphical Abstract/Table of contents entry



Text:

Immersion of capacitive electrodes into a multiple-chamber bioelectrochemical reactor substantially increased energy capture from synthetic river water and seawater.